

Supporting Information

Phosphoric acid functionalized pre-sintered *meso*-silica for high temperature proton exchange membrane fuel cells

Jie Zeng,^a Beibei He,^a Krystina Lamb,^b Roland De Marco,^b Pei Kang Shen,^c San Ping Jiang,^{*a}

Experiments and characterization

The synthesis of mesoporous silica was based the procedures reported in the literature.¹⁻⁴ Pluronic surfactant and hydrochloric acid were dissolved in deionized-water according to a certain ratio. Then, butanol was added at 45°C and after stirring for 1 h, tetraethylorthosilicate (TEOS, Sigma-Aldrich) was added; the synthesis was carried out in a hydrothermal reactor. The mixture was further stirred vigorously at 45°C for 24h and subsequently was aged at 100°C for 24 h; then the mixture was dried at room temperature for 24h. The powder was calcinated at temperatures range of 550°C for 6h and N₂ was used as protective gas at temperature below 200°C. The as-prepared meso-silica powder was mixed with PVA binder (5wt%) and the die pressed to form meso-silica discs. The discs were then sintered at temperature range of 550 to 850°C. The sintered meso-silica discs were then polished to thickness of 0.2 to 0.5 mm and impregnated in a 83%wt phosphoric acid (PA) solution for 24 h, forming PA-functionalized meso-silica (PA/*meso*-silica) membranes

Small angle X-ray scattering (SAXS) spectra were carried on a SAXSess high-flux small-angle X-ray scattering instrument (AntoPaar GmbH) equipped with two-dimensional wire detector and a Cu ($\lambda=0.1542\text{nm}$) rotating anode operated at 80 kV and 40 mA. Nitrogen adsorption/desorption isotherms were measured using a Micromeritics ASAP Tristar II 3020 system. Specific surface area was calculated using the Brumauer-Emmett-Teller (BET) method. The total pore volumes were estimated from the adsorbed amount at the relative pressure of $P/P_0=0.95$ and the pore size distributions were obtained from the adsorption branch of the isotherms by using the non-linear density function theory (NLDFT) method. TEM micrographs were obtained using a JSM-2100F JEOL electron microscope equipped with EDX-detector (Noran Instr.) and operated at 200 kV with a cold-field emission source. TGA was carried out on a TG/DTA Q500 from 30 to 500 °C at a heating rate of 10 °C min⁻¹ under nitrogen flow of 40 ml min⁻¹. FTIR absorption spectra of the PA/*meso*-silica composite membranes were recorded with a JASCO FTIR-Q250 spectrometer (spectral range of 4000-200 cm⁻¹, 50 scans, and a resolution of 1 cm⁻¹).

The membrane-electrode-assembly (MEA) based on PA/*meso*-silica membrane disc was assembled. The PA/*meso*-silica disc was 5cm in diameter and 220 μ m in thickness. A mixture of PtRu/C catalyst (40% Pt and 20% Ru on Vulcan XC-72R Carbon, Johnson Matthey), Nafion solution (5 wt % in a mixture of aliphatic alcohols, Sigma Aldrich), and isopropyl alcohol (Sigma-Aldrich) was sprayed onto a carbon gas diffusion layer (Toray Graphite Paper, TGPH-120, 40% wet-proofed, E-TEK, Inc.) by airbrushing until a platinum loading of 3 mg cm⁻² was achieved for the anode. The same procedure was used for the cathode with Pt loading of 2 mg cm⁻² (60% Pt on Vulcan XC-72R Carbon, Johnson Matthey). The electrode area was 4.0 cm². Methanol fuel was pumped with a peristaltic pump and the methanol flow rate of 2 mL min⁻¹ was regulated with a recirculation loop and measured by a flowmeter (Alicat Scientific) before being fed into a vaporizer. The steam generated in this way entered the anodic compartment of the DMFC.

Proton conductivity measurements of PA/*meso*-silica membrane disc were performed by a four-probe method, using electrochemical impedance spectroscopy (PGSTAT30/FRA, Autolab, Netherlands) over the frequency range from 1Hz to 1MHz. In the temperatures range from 75 to 225 °C, the conductivity of PA/*meso*-silica membrane was measured with no external humidification. For the purpose of comparison, Nafion 117 membrane was also measured and in the temperature range of 25-80°C the relative humidity (RH) of the measurements was controlled by a PEMFC test station (FCATS-G050, Greenlight, Canada). The cell performance was measured with the methanol flow rate of 2 mL min⁻¹ and the O₂ flow rate of 40mL min⁻¹. No back pressure control of both sides in this work.

Additional Results

Figure S1 is the SAXS spectra of *meso*-silica membrane discs sintered at different temperatures. The sample before sintering show well-resolved scattering peaks and characteristic SAXS patterns of *Ia $\bar{3}d$* symmetry⁵, suggesting the successful formation of the well-ordered *Ia $\bar{3}d$* mesoporous structure. The increase of sintering temperatures from 550 °C to 750 °C caused a pronounced shift of the characteristic SAXS peaks towards higher angles, an evidence for the contraction of unit cell parameter (α) of the mesoporous silica from 24.2 nm to 21.9 nm. It is also noted that the intensity of major SAXS peaks were firstly enhanced for *meso*-silica treated at higher temperatures and reached a peak value at 650 °C, the peak intensity decreases significantly as sintering temperature increases to 750 °C. At a sintering temperature of 850°C, the peak (211) disappeared completely. This indicates that the ordered

structure of mesoporous silica is stable at sintering temperature 650 °C and becomes disordered at sintering temperatures 750 °C or higher.

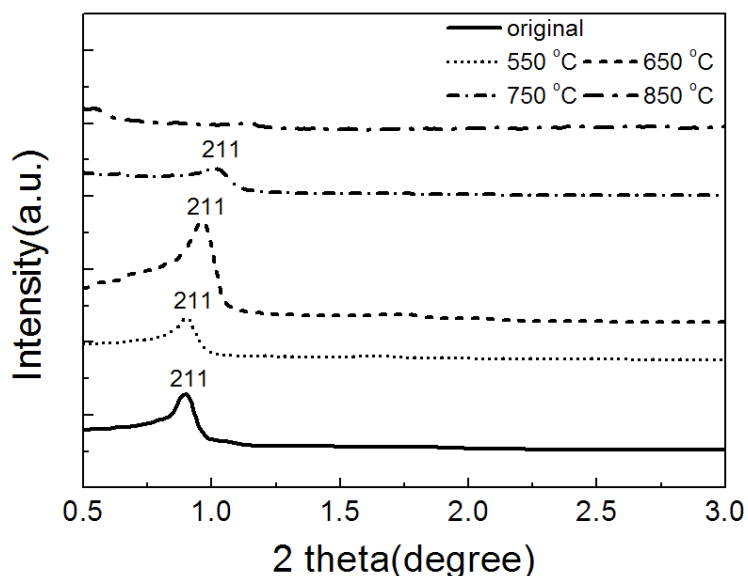


Figure S1. Small-angle X-ray scattering patterns of mesoporous silica disc sintered at various temperatures from 550 to 850 °C.

The porosity and BET surface areas of original and sintered meso-silica were measured by nitrogen absorption. The N₂ sorption isotherms feature typical type-IV associated with a distinct step at relative pressure of ~0.7 that is attributed to nitrogen condensation in narrow size distribution mesopores for all samples except meso-silica sintered at 850 °C (meso-silica-850). The results show that for meso-silica sintered at 650 °C, the mesopore diameter is 8.2 nm, similar to that measured on meso-silica powder before sintering (see Table S1).

Table S1. Textural parameters of mesoporous silica family and the inclusion compound

Samples	Unit cell α (nm) ^a	S_{BET} (m ² g ⁻¹)	Pore vol (cm ³ g ⁻¹) ^b	Poresize (nm) ^c	Wall thickness (nm) ^d
Meso-silica (before sintering)	24.2	913	1.146	8.2	5.0±0.2
Meso-silica-550	24.0	936	1.238	8.2	4.8±0.2
Meso-silica-650	22.6	948	1.312	8.2	4.2±0.2
Meso-silica-750	21.9	522	0.488	8.0	3.9±0.6
Meso-silica-850	N.A.	87	0.131	N.A.	N.A.

^a Calculated from SAXS results

^b Cumulative pore volume

^c Calculated from the adsorption branch of the isotherms based on the NLDFT method

^d Estimated from SAXS and BET results

The thermal properties of nonporous silica based and mesoporous silica based membranes are assessed with TGA (**Figure S2**). In the case of *meso*-silica, the weight loss mainly occurs

at temperature around 60 °C, which is attributed to the dehydration of adsorbed water. The dry meso-silica membrane contains ca. 1.2 wt % water, compared to ca. 26 wt % for the fully hydrated mesoporous silica.

On the other hand, the mesoporous silica/PA membrane exhibit two distinct weight loss processes in temperature range of 30-800 °C. The first weight loss start from ambient temperature to 100 °C is mainly attributed to absorbed water from the doping phosphoric acid solution and some less stable phosphoric acid on the membrane surface. The second loss centered at around 200 °C is assigned to the evaporation of phosphoric acid. The high doping level of H₃PO₄ in meso-silica/PA reflected in the total weight loss of 38 % at 800 °C, which ascribed to the dehydration of doped PA solution. The high doping level reflects the large pore volume of the meso-silica membrane.

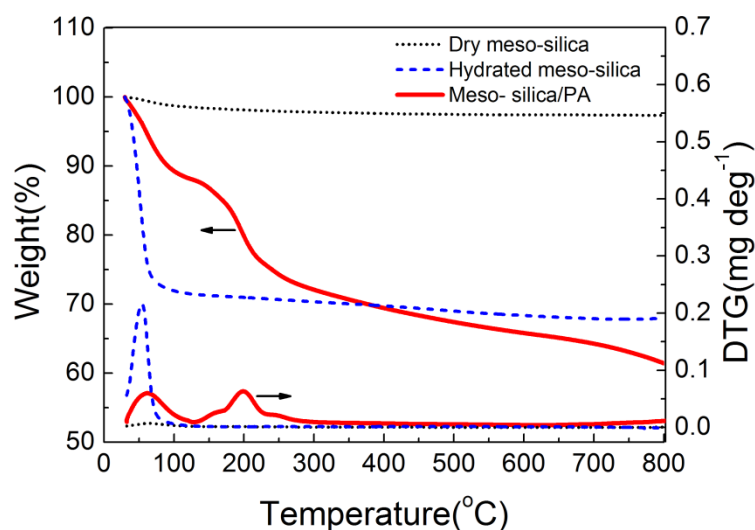


Figure S2. Thermogravimetric analyses (TGA) of dry meso-silica membrane, hydrated meso-silica membrane and meso-silica/PA membrane; the numbers showed in the figures give the weight loss percentage at 200°C.

Figure S3a is the FTIR spectra of mesoporous silica and PA/meso-silica. A weak band at 1612 cm⁻¹ can be ascribed to the O-H vibration of adsorbed water; in addition, a broad band at 801 cm⁻¹ is observed, which is the characteristic of the vibrations of Si-O-Si.⁶ The FTIR spectra of H₃PO₄-doped meso-silica before and after ageing in PA solution showed the characteristic peaks of phosphoric acid moiety; δP=O and δP-O appeared at 951 and 894 cm⁻¹, respectively, besides, the couple bands at 1050 and 765 cm⁻¹ are assigned to the in-plane and out-of-plane bending modes of P-O-H, respectively.^{7,8} These indicate the success of immobilization process. The spectra also observed a significant shift of O-H vibration of adsorbed water from 1612 to 1634 cm⁻¹, which results from the protonation of water within the membrane.

The Raman scattering spectra of meso-silica, meso-silica/PA and aged meso-silica/PA membranes are given in **Figure S3b**. Compared with the spectrum of un-doped meso-silica membrane, significant difference can be observed in the spectra of meso-silica/PA membranes. The very strong bands appear at 900 cm^{-1} can be ascribed to the P-O stretching of H_3PO_4 , the O-H stretching leads to another strong band at 2026 cm^{-1} . Besides, the bands at 376 and 488 cm^{-1} is assigned to the vibration mode of P-O in the phosphate group, which indicates the formation of P-O-P and/or Si-O-P bonds in the composite PA/meso-silica membrane.

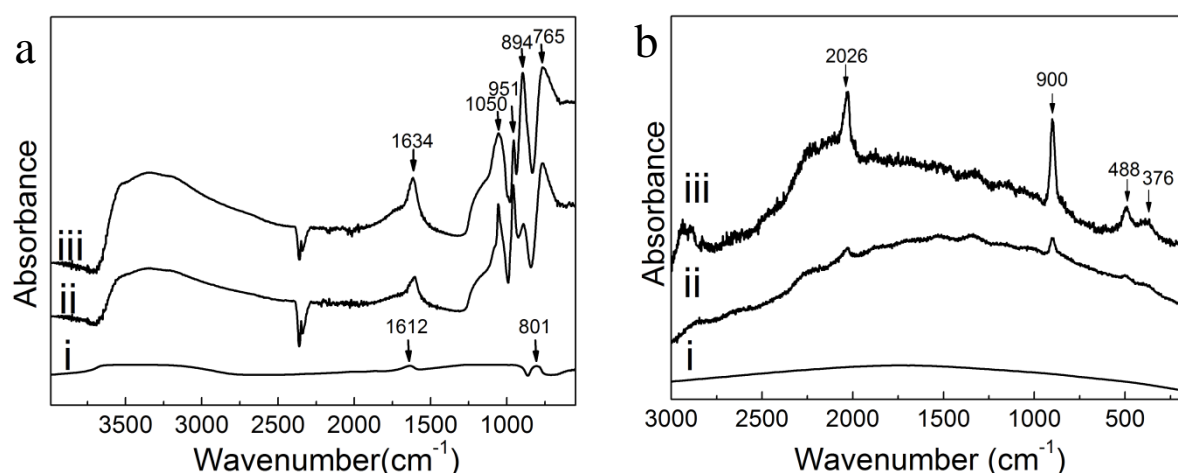


Figure S3. (a) FTIR and (b) Raman spectra of (i) meso-silica membrane, (ii) meso-silica/PA membrane, (iii) and meso-silica/PA membrane aged in phosphoric acid for 8 months .

References:

1. F. Kleitz, D. Liu, G. M. Anilkumar, I.-S. Park, L. A. Solovyov, A. N. Shmakov and R. Ryoo, *The Journal of Physical Chemistry B*, 2003, **107**, 14296-14300.
2. F. Kleitz, S. H. Choi and R. Ryoo, *Chemical Communications*, 2003, 2136-2137.
3. F. Kleitz, L. A. Solvyov, G. M. Anilkumar, S. H. Choi and R. Ryoo, *Chemical Communications*, 2004, 1536-1537.
4. D. H. Chen, Z. Li, C. Z. Yu, Y. F. Shi, Z. D. Zhang, B. Tu and D. Y. Zhao, *Chem. Mat.*, 2005, **17**, 3228-3234.
5. Y. Wan and D. Y. Zhao, *Chem. Rev.*, 2007, **107**, 2821-2860.
6. W. J. Liang, S. J. Hsieh, C. Y. Hsu, W. F. Chen and P. L. Kuo, *Journal of Polymer Science Part B-Polymer Physics*, 2006, **44**, 2135-2144.
7. A. M. Donia, A. A. Atia, A. M. Daher and E. A. Elshehy, *Journal of Dispersion Science and Technology*, 2011, **32**, 193-202.
8. B. Boonchom, C. Danvirutai, S. Youngme and S. Maensiri, *Industrial & Engineering Chemistry Research*, 2008, **47**, 7642-7647.